Two-dimensional soil water evaporation in hedgerow orchards

by

Ndivhudzannyi Sylvester Mpandeli

Presented in partial fulfillment of the requirements for the degree

M. Inst. Agrar. (Agronomy)

IN THE FACULTY OF NATURAL AND AGRICULTURAL SCIENCES

DEPARTMENT OF PLANT PRODUCTION AND SOIL SCIENCE

UNIVERSITY OF PRETORIA

Supervisor: **Prof. J. G. Annandale**

Co-supervisor: **Dr .P. Lobit**

September 2001

Abstract

The Soil Water Balance two-dimensional model is a daily time step model that simulates canopy radiation interception across the row. The purpose of the experiment was to obtain the data necessary to validate the model.

Solarimeter tubes and micro-lysimeters were installed across a row in a peach orchard and measurements were taken for six days. Spatial patterns of daily cumulative radiation interception on the soil varied with position across the row. Sites under the trees and on the northern side of the row received more radiation than those on the southern side. The evaporation pattern appeared to match that of solar radiation interception, with most of the evaporation occurring on the northern side of the row.

The two-dimensional energy interception and soil evaporation components were validated separately. The radiation interception model predicted generally quite well soil irradiance measured with tube solarimeter at different distances across the row. Model simulations of radiation interception fitted the measurements well, though dimensions of the tree canopy had to be adjusted to correctly estimate evaporation. Assuming a 30% air humidity instead of 50% (default value in the model) led to a better estimation of evaporation.

Acknowledgements

It is with heartfelt gratitude that I acknowledge the following people:

Prof .J. G. Annandale, my supervisor, for providing direction, support and guidance. Thank you for being patient and understanding. I learnt a lot from you now have a clear understanding of what it takes to do good research work.

Dr .N. Z. Jovanovic and **Dr .P. Lobit**, my co-supervisors, for your invaluable advice, support and interest in this project.

Water Research Commision, for their contribution and financial support, and for making this project possible.

Table of contents

Chapter 1 1
1.1 Introduction 1
1.1.1 Theoretical background 1
1.1.2 The SWB model 2
1.1.3 In-situ evaporation measurements 3
Chapter 2 5
2.1 Material and Methods 5
2.1.1 Site description and environmental conditions 5
2.1.2 Training system and tree dimensions 5
2.1.3 Weather variables 6
2.1.4 Solarimeters 6
2.1.5 Micro-Lysimeters 6
Chapter 3 10
3.1 Results and discussion 10
3.1.1 Energy interception measurements 10
3.1.2 Analysis of the micro-lysimeter technique 14
3.1.3 Lysimeter measurements in the orchard 16
3.1.4 Validation of the evaporation subroutine 18
Chapter 4 26
4.1 Conclusion 26
4.1.1 General comparison between measurements and model predictions 26
4.1.2 Perspective 27
References 28
Appendix 1: Wiring table of the seven solarimeter tubes 31
Appendix 2: Logger program of the solarimeter tubes 32
Appendix 3: Wiring table of the automatic weather station 35
Appendix 4: Logger program of the automatic weather station 36
Appendix 5: Weather data 40

Chapter 1

1.1 Introduction

The interest in crop modelling started since the introduction and popularisation of computer technology, which facilitated the dynamic simulation of complex natural systems (Sinclair and Selisman, 1996). Crop growth and soil water balance models for irrigation scheduling are popular at locations where water is a limiting factor for crop production (Bennie et al., 1988, Smith, 1992b, Crosby, 1996, Annandale et al., 2000). This is particularly true for fruit crops due to their importance on the export and local markets. Hedgerow tree crops are planted in widely spaced rows to allow access between trees to carry out necessary management practices for example pest control and harvesting. Distribution of energy is therefore not uniform in widely spaced crops. A one-dimensional assumption could lead to serious inaccuracies caused by adjacent row shading, which depends on solar and row orientation, tree size and shape. In addition, localised under-tree irrigation is often used for tree crops to maximize irrigation efficiency. This irrigation (micro or drip) only wets a limited area under the canopy of the trees so that evaporation from the soil surface is also not uniform. It is essential to take into account the limited volume of soil wetted under micro-irrigation or its capacity will easily be exceeded with a standard one-dimensional approach, leading to undesirable over irrigation in the wetted zone, and possibly crop stress due to a long an irrigation interval. In order to accurately estimate canopy growth, water balance and yield, it is therefore essential to model canopy radiant interception and soil water balance of hedgerow tree crops in two dimensions and on an hourly time step, based on sound physical principles.

1.1.1 Theoretical background

The rate of evaporation from a crop is dependent on meteorological conditions such as wind speed, relative humidity, temperature and solar radiation (Penman, 1948). When crops are grown in a row configuration, the crop canopy may not completely cover the soil, and the exposed soil may receive an important proportion of the incident solar radiation, as well as evaporate significant amounts of water (Ham et al., 1991). Crop canopies intercept radiation thus reducing the energy available for the evaporation process (Allen et al., 1964). Thus, investigating evaporation in a row crop

system requires that both the soil and canopy be examined (Tanner and Jury, 1976; Shuttleworth and Wallace, 1985; Lascano et al., 1987). This is particularly true for tree orchards, in which widely spaced rows bring large diurnal changes in exposure of plants and soil to solar radiation.

1.1.2 The Soil Water Balance model

A two-dimensional model of energy interception and soil water balance has been developed to predict water use in row crops and orchards. It is derived from the SWB model, described in Annandale et al. (2000). The SWB model, initially designed to model the crop cover in one dimension, was modified to include a two-dimensional description of radiation interception by the canopy, evaporation, and water movement in the soil.

In simulating crop growth and the field soil water balance, many models use canopy radiant interception for two purposes (i) To determine the photosynthesis rate and dry matter production from the amount of energy intercepted by the crop canopy (Monteith, 1977) and (ii) To estimate soil water evaporation and crop transpiration from the amount of energy available for these two processes (Ritchie, 1972). Canopy radiant interception represents the fraction of solar radiation available to the crops. The distribution of light within the tree canopy is equally important for fruit production since it can affect flowering, fruit size, fruit colour and other quality factors (Doud and Ferree, 1980, Morgan et al., 1984). The two-dimensional energy interception model assumes leaves to be uniformly distributed within an ellipsoid, and radiation penetrating the canopy to be attenuated according to Beer's law. The radiation interception model described here is based on the work of Charles-Edwards and Thornley (1973) and Charles-Edwards and Thorpe (1976). In order to determine the spatial distribution of soil irradiance across the tree row, the canopy path length through which the radiation must travel to reach a certain point on the soil surface is calculated. Beam or direct radiation and diffuse radiation for the PAR (photosynthetically active radiation) and NIR (near-infrared radiation) wavebands are calculated separately as they interact differently with the canopy. The attenuation of beam radiation by the canopy is a function of zenith angle, azimuth angle and row orientation. Elevation and azimuth angles are calculated from latitude, solar declination that depends on day of year, and time of day.

Evaporation is calculated as follows: potential evapotranspiration (PET) is calculated from weather data using the FAO Penman-Monteith equation (Allen et al., 1998) and the maximum crop factor after rainfall occurs. At each node on the soil surface, local PET is recalculated as PET weighed by the fraction of total radiation received at this point. Actual evaporation is computed as a proportional to local PET and to the gradient of humidity between the soil surface and the atmosphere.

Water redistribution in the soil and humidity at the soil surface are calculated by computing two-dimensional soil water movement, using a finite difference model. A grid of nodes is established, that divides the soil into a number of elements. Each element has its own physical properties, so this scheme allows variation in soil properties in two dimensions. The model redistributes water in the soil in two-dimensions using a finite difference solution to Richards' continuity equation for water flow.

1.1.3 In-situ evaporation measurements

The validation of the "Tree" version of the SWB model requires measurements of : (i) Tree dimensions and canopy characteristics, (ii) Energy interception at the soil surface, (iii) Water evaporation from the soil surface. While the first two points do not pose particular problems; evaporation measurements are more difficult.

One technique available to measure evaporation is micro-lysimeters: it consists of measuring the mass loss of a small volume of wet soil in a container at the soil surface (Shawcroft and Gardner, 1983). The technique has been used extensively for measuring evaporation from bare soils (Caprio et al., 1985, Lascano and Van Bavel, 1986).

However, the practical use of micro-lysimeters is subject to several restrictions. Previous research showed that the rate of evaporation measured with micro-lysimeters and other techniques did often not match very closely. For example, Boast and Robertson (1982), Matthias, et al. (1986) and Steiner (1989) found that the measured crop total evapo-transpiration exceeded the sum of plant transpiration and soil surface evaporation (measured using micro-lysimeters). One condition for the micro-lysimeter to give accurate measurements of evaporation is that the soil in the micro-lysimeter must be representative of the rest of the orchard. However, installing the lysimeter without disturbing the soil, as Boast & Robertson (1982) proposed, is

practically impossible. As a consequence, Shawcroft and Gardner (1983) found that the conditions inside the isolated micro-lysimeters were different from those of the surrounding soil. Also, the interpretation of evaporation measurements made with micro-lysimeters is often difficult. One of the problems is that significant drying of the soil surface usually occurs when the evaporation rate from the surface layer exceeds the rate of water movement toward the surface from the underlying soil layers.

Since evaporation depends on the soil surface water content (Black et al., 1970) the rate of evaporation measured with the micro-lysimeter changes over time: after an wetting event, the soil surface is wet and the evaporation is limited by the net radiation received. Then the supply of water by the soil to the surface becomes limiting and evaporation decreases as the soil becomes drier. Therefore, two stages can be distinguished: the first one is called energy- or demand-limited, whereas the second one is water- or supply- limited. This behaviour, already reported in previous lysimeter studies (Phillip 1957, Black et al. 1969), was modelled by Ritchie (1972). This model has since then been widely adopted in various lysimeter studies (Villalobos and Fereres 1990, Yanusa et al. 1993).

Theoretical approaches have also been developed to describe and quantify the evaporation process. They are based on the notion of energy fluxes: evaporation being determined by the amount of energy supplied to bring water from the liquid or bound phase to the vapour phase and it can be quantified by estimating heat fluxes. These studies have provided some hints to explain the discrepancies in experimental measurements. Walker (1984) measured evaporation from a wet soil under a row crop and found that the latent heat flux often exceeded the available radiative energy, suggesting that sensible heat transport from the crop to the soil was influencing evaporation. On the contrary, by examining the within-canopy profiles of heat and water vapour, Begg et al. (1964), as well as Brown and Covey (1966) concluded that there was a sensible heat flux from the soil and lower leaves to the top of the canopy. Similar observations were reported by Tanner (1960) and Fuchs (1972).

The objectives of this trial were: (i) To establish the daily and spatial patterns of radiative energy interception at the soil surface under the orchard, (ii) To measure the spatial distribution of evaporation in the orchard, (iii) To use these data to validate the SWB model for orchards, in particular the procedures concerning radiation interception and evaporation.

Chapter 2

2.1 Material and Methods

2.1.1 Site description and environmental conditions

This study was conducted in a peach field trial during the 2001 seasons at the Hatfield experimental farm, South Africa (25° 64´S, 28°16 E, Altitude 1372 m). This is a summer rainfall region (October-March) with an average of 670 mm year^{-1}. The monthly average maximum temperature is 30°C (January), with a monthly average minimum of 1.5°C (July). Frost occurs during winter.

The soil is a sandy loam (28% clay, 10% silt and 62% sand) Hutton (Soil classification Working Group, 1991) with depths generally in excess of 1.2 m (a small portion having scattered hard plinthic formations at 1.1 m^2). Soil analysis revealed adequate P(120 mg /kg^{-1}), pH (H_20) being 6.4 and sufficient Ca, Mg & K (580, 140 and 160 mg/ kg).

The orchard was divided into two sections: one with grass cover, the other with bare soil. The day during the experiment commenced, irrigation was applied using a sprinkler irrigation system to ensure a uniform wetting.

2.1.2 Training system and tree dimensions

The orchard was planted in 4.5 m rows, oriented East to West (Figure 1). The trees were planted in 1994, and trained as an open vase.

Tree dimensions were measured using a 5 m ruler. One person held the ruler while another one was standing about 5 m from the orchard and measuring the dimensions. Tree height, i.e. the height of the end of the top shoot, was almost the same for all the trees, between 3.70 m and 3.80 m. Width was 4.20 m, corresponding to the maximum extension of the branches. Most of the canopy, however, was enclosed within a smaller width, but it was difficult to estimate a value for it because of the branches masking each other. Bare stem height (0.45 m) is the distance from the soil to the lower branches of the tree. Again, it did not exactly reflect the position of the base of the foliage, since the lower branches bore very few leaves, the bottom of the volume that enclosed most of the canopy was higher value.

2.1.3 *Weather variables*

An automatic weather station located 200 m away from trial was used to measure weather variables. The data were collected and recorded hourly by a CR10X datalogger (Campbell Scientific Inc., Logan, Utah, USA). The following variables were measured.

- Solar radiation (Wm^{-2}) with an LI 200X pyranometer (LI-COR, Lincon, Nebraska, USA).
- Temperature (°C) and relative humidity (%) with an HMP35C sensor.
- Wind speed ($m\ s^{-1}$) with a propeller anemometer sensor.
- Rainfall (mm) was measured with a electronic raingauge.

The datalogger was programmed to automatically calculate hourly average vapour pressure(kPa), saturation vapour pressure (kPa) and vapour pressure deficit (kPa).

2.1.4 *Solarimeters*

Solar radiation interception at the soil surface was measured using seven tube solarimeters (Delta- T Devices Ltd, Burwell, Cambridge, England) positioned under the canopy of the peach trees in the inter- row region, at distances ranging from approximately 2 m on the southern side to 2 m on the northern side of the row (Figure 1). The tube solarimeters were set up parallel to the tree row (Figure 2).

The solarimeters were calibrated against the pyranometer at the weather station. The solarimeters were coupled to a CR10X datalogger (Campbell Scientific, Logan, Utah, USA). Measured values were averaged at ten seconds intervals and recorded every 5 minutes.

2.1.5 *Micro-Lysimeters*

Evaporation from the soil surface was measured using the micro-lysimeter method (Boast and Robertson, 1982).

In this experiment, the micro-lysimeters were made out of PVC pipes 300 mm length with a 110 mm internal diameter and 3.5 mm wall thickness. The micro-lysimeters were made as follows: PVC tubes were hammered into the soil in a portion of the orchard where the soil had been irrigated: in this way, tubes filled with an undisturbed core of soil were obtained. The tubes were then carefully twisted and dug out of the

soil, leaving the soil core inside intact. The base of the tubes was then closed with a plastic cap. Holes were made in the orchard at the positions where the lysimeters were to be installed, and the tubes were inserted in the holes to a depth at which the upper rim was level with the soil surface, so as not to alter the wind regime above the soil surface (Figure 3).

Evaporation measurements were made by weighing the micro-lysimeters daily. Measurements were taken using an electronic scale (Figure 4), and the average value was used (in a few cases, discrepancies between these consecutive measurements led to discarding one of them). Evaporation (mm day^{-1}) was calculated as the mass difference between two days, divided by the product of the density of water and the area of the tube.

Experiment 1

The main experiment with micro-lysimeters consisted of measurements of evaporation in the orchard. Nineteen micro-lysimeters were installed perpendicular to the rows of the orchard, at distances ranging from 0 to 2.5 m on either side of the row (Figure 1). Eleven of them had a bare soil surface and were installed in a row where the soil was kept bare, and eight others had a grass covered surface and were installed in a grass-covered area. After an initial irrigation of 20 mm, applied with sprinklers, soil water evaporation was measured for six days (05-12/03/2001, DOY 64 to 71).

Experiment 2

Another experiment was conducted to check that the micro-lysimeters give consistent estimates of evaporation and to check how they work with different soil samples. We assumed that the FAO Penman-Monteith equation (Allen et al., 1998) gives a reasonable estimate of potential evaporation. The experiment consisted of measurements of soil water evaporation from eight micro-lysimeters installed in an open field close to the weather station. Four of these micro-lysimeters had a bare soil surface and were located in a bare soil area, and the other four had a grass covered surface and were in a grass covered area. These measurements went on for seven days after an initial irrigation of 20 mm, applied with the same sprinkler system as for the peach Orchard, evaporation was measured for seven days (04/04/2001-11/04/2001, DOY 94 to 100).

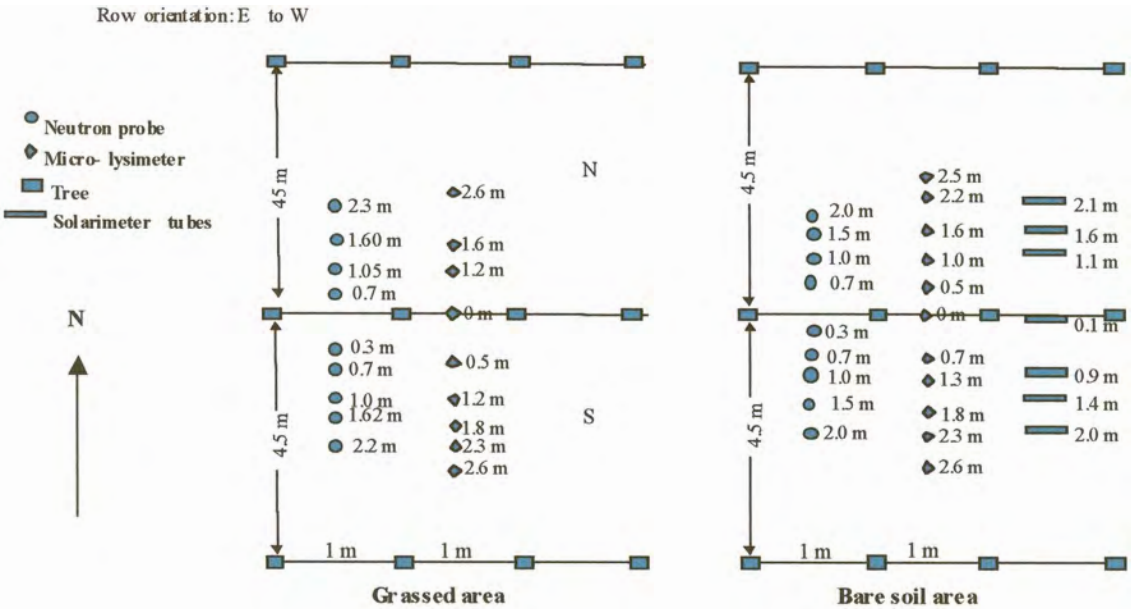

Figure 1. Map of the experimental orchard and equipment installed.

Figure 2. Equipment installed in the peach site: micro-lysimeters and solarimeter tubes.

Figure 3. The lower part of the picture shows the pre-formed hole in which the micro-lysimeter is to be installed and the steel cylinder used to prepare the pre- formed hole. The upper part shows a the micro-lysimeter installed

Figure 4. Weighing of the micro-lysimeters. The cylinders are cleaned before weighing.

Chapter 3

3.1 Results and discussion

3.1.1 Energy interception measurements

These data were used: (i) To investigate the daily patterns of radiation interception at the soil surface and (ii) To quantify the cumulative amounts of solar radiation received daily at different positions in the orchard. These data were used to check the validity of the geometry used to describe tree shape used to predict radiation interception, and to validate the estimations of cumulative energy used for the evaporation part of the model.

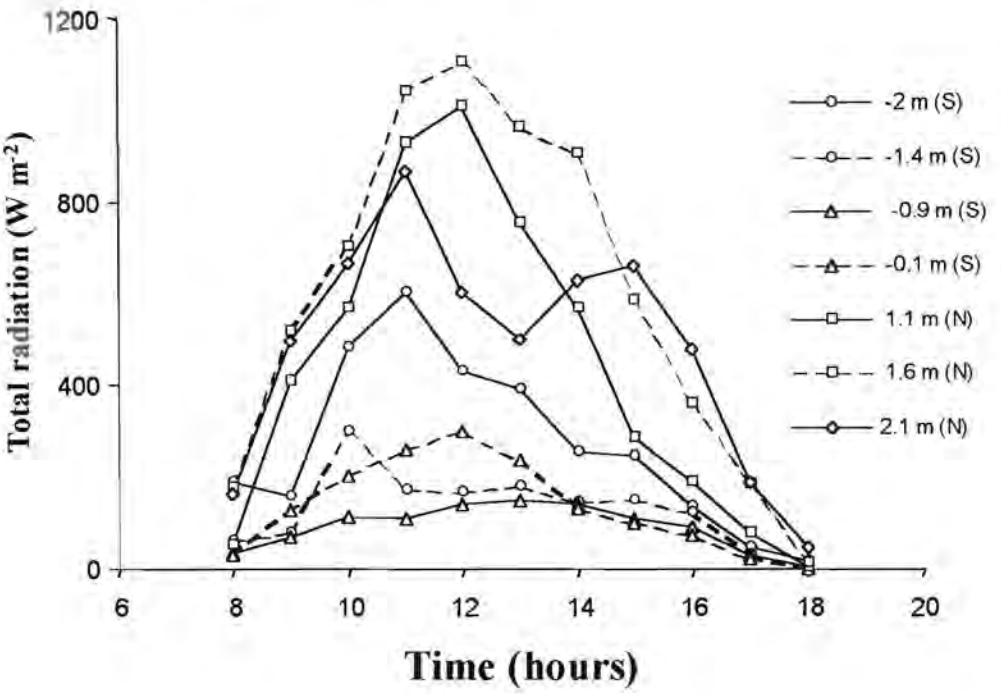

Figure 5. Daily patterns of energy interception at different distances from the row, ranging from -2 m (southern side) to 2.1 m (northern side) observed on the first day of the experiment. Radiation received at the soil surface is expressed in W m^{-2}.

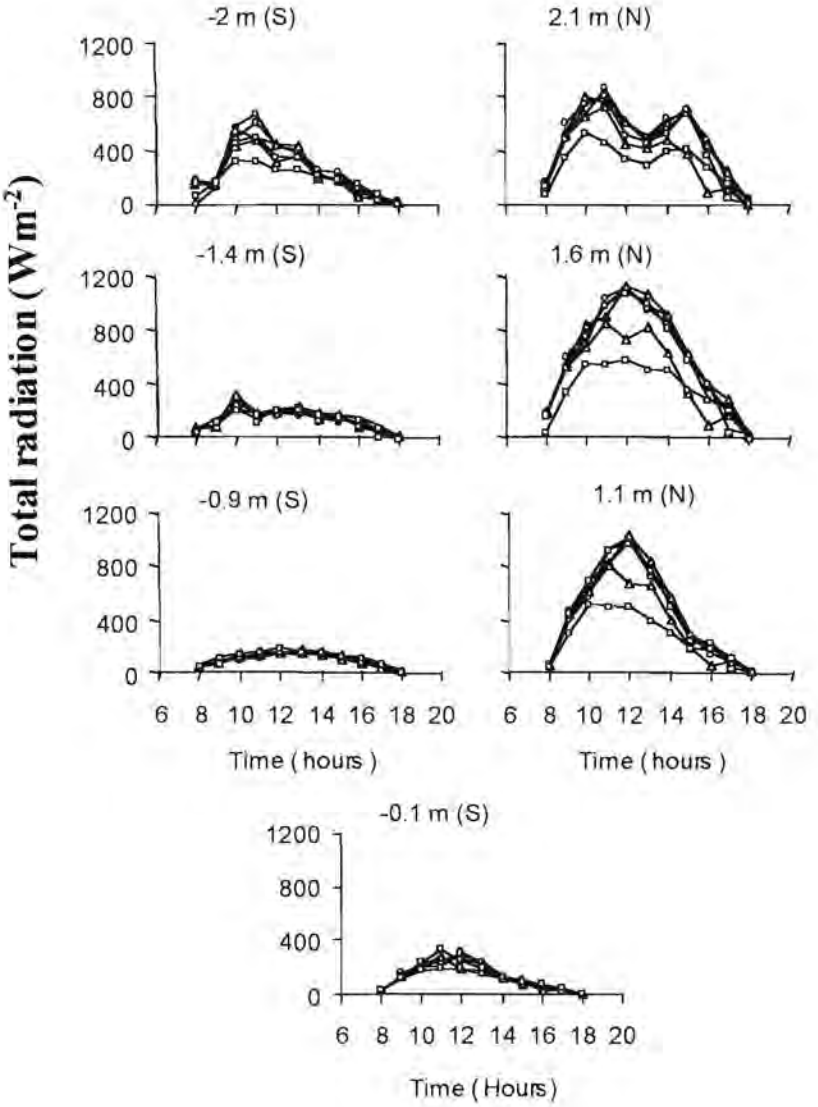

Figure 6. Daily patterns of energy interception at different distances from the row, ranging from -2 m (southern side) to 2.1 m (northern side). Each graph represents the radiation received at the soil surface (expressed in Wm^{-2}) at a given distance from the row, for the six days of the experiment.

The flux of solar radiation reaching the soil depended on the time of the day and on the position in the orchard (Figures 5 and 6). At 0.9 and 1.4 m on the southern side of the tree, the radiation received at the soil surface was low throughout the day (about 200 W m^{-2}). On the contrary, on the northern side of the tree there was almost full exposure to solar radiation at some times of the day (with about 1000 W m^{-2} between 10:00 and 12:00 at 1.1 m, and between 9:00 and 13:00 at 1.6 m). Positions mid way

between the rows exhibited an intermediate behaviour, with a peak of about 800 W m^{-2} radiation in the morning at 2 m and two peaks of about more 600 W m^{-2} at 2.1 m, one in the morning and one in the afternoon.

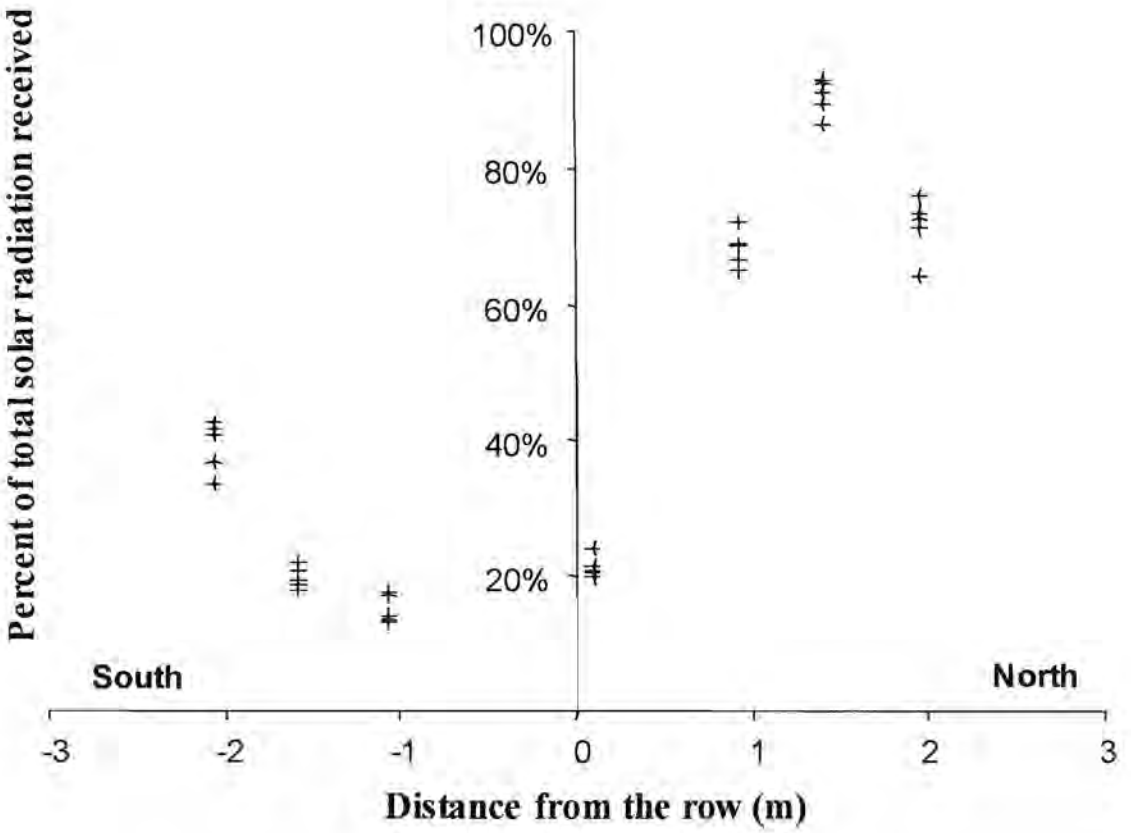

Figure 7. Distribution of total fraction of amount of energy received daily by solarimeter tubes at different positions under the canopy of the trees (percent of total radiation). The negative values represent the southern sides and the positive values are for the northern sides of the tree row.

Differences in daily patterns of energy interception between positions explained the differences in the distribution of daily cumulative energy interception (Figure 7). Positions between approximately 0 and -2 m on the southern side of the tree received the lowest level of daily cumulative energy (about 15% of total solar radiation), whereas the highest levels were received between 1 and 2 m on the northern side (with about 90% of solar radiation reaching the soil). This pattern is similar to that described by Pruitt et al. (1984).

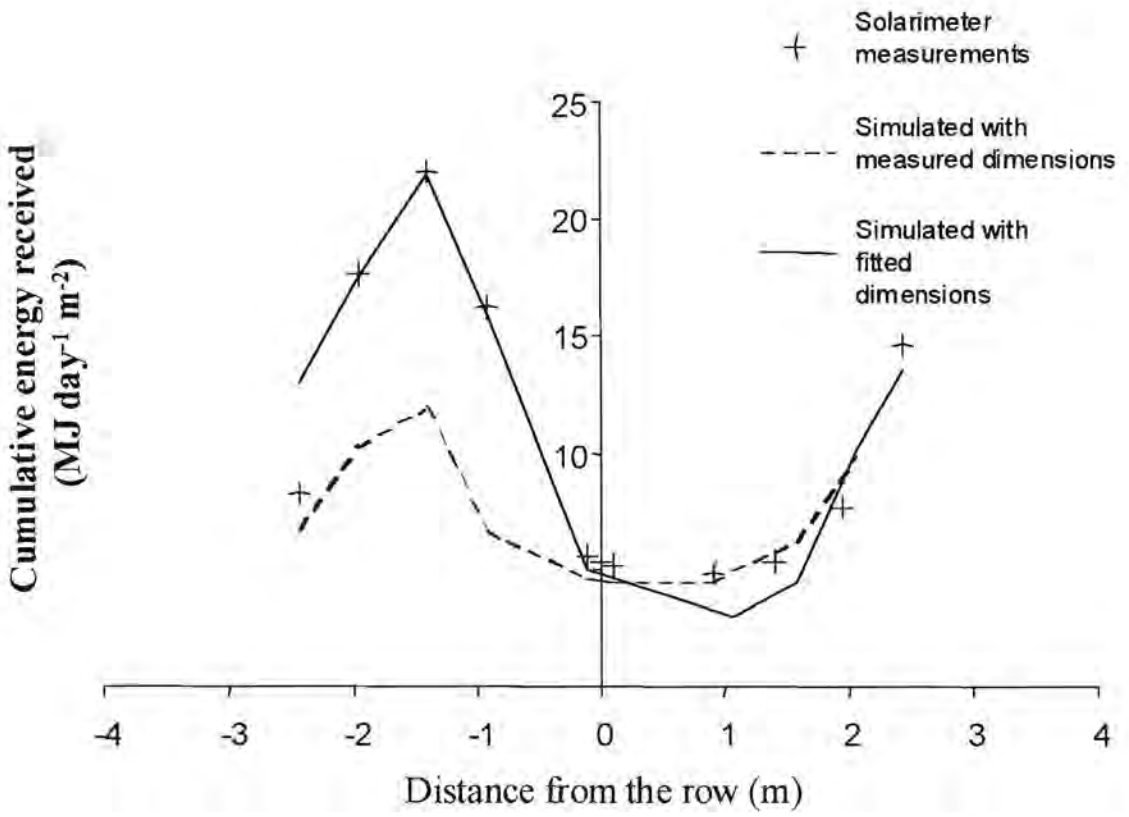

Figure 8. Comparison between distributions of energy at the soil surface measured and simulated with the model during the first day of the experiment (DOY 64, 05/03/2001). The measured dimensions of the tree were: height 3.76 m, width 4.2 m and bare stem height 0.45 m. The best fit was obtained for the following tree dimensions: height 3.76 m, width 3.8 m and trunk height 0.9 m.

Simulations were run with the SWB model to validate the predictions of cumulative daily energy interception. The parameters of the model that can be adjusted are the tree dimensions (height, width and bare stem height), and the physical values associated with radiation extinction through the canopy (leaf area density, extinction coefficient and absorptivity). Several simulations were run with different sets of parameters showed that changing tree dimensions affected the shape of the curve of radiation distribution, whereas changing the parameters associated with radiation extinction led to distributions with similar shapes but different magnitudes.

Using the measured values for tree size (height 3.76 m, width 4.2 m, trunk height 0.45 m), and the following coefficients: leaf area density 1.2 m^{-1}, extinction coefficient 0.5, and absorptivity 0.5, did not give satisfactory description of energy distribution.

Cumulative radiation was underestimated by about half on the northern side of the row, and the size of the shaded area was over-estimated (Figure 8). Adjusting these last three parameters did not help to better predict the shape of the distribution. The best prediction of energy distribution was obtained with the following parameters: height 3.76 m, width 3.8 m, trunk height 0.90 m, leaf area density 1.2 m^2 leaves m^{-3} canopy, extinction coefficient and absorptivity 0.5 (Figure 8). This was the best prediction of radiation interception obtained with trees 40 cm narrower, and with the bottom of the canopy 55 cm higher than measured.

Concerning the width of the tree, this is probably due to the fact that the canopy was not exactly ellipsoidal though the trees had rather few leaves, some scaffold branches at the base extended further than the rest of the canopy. Therefore, the tree width measured in the orchard did not properly reflect the average boundaries of the canopy. Concerning the bare stem height, the bias in its estimation was probably related to an irregular distribution of the leaf density: the branches originating from the base of the trunk bear fewer shoots and leaves than the rest of the canopy, so that in terms of interception it occurred as if the base of the canopy was higher than measured.

3.1.2 Analysis of the micro-lysimeter technique

In order to test the micro-lysimeters as a tool to measure evaporation, eight of them were in an open field, and measurements taken for 6 days. The measured evaporation was compared to the grass reference evapo-transpiration (*ETo*) calculated using weather station data.

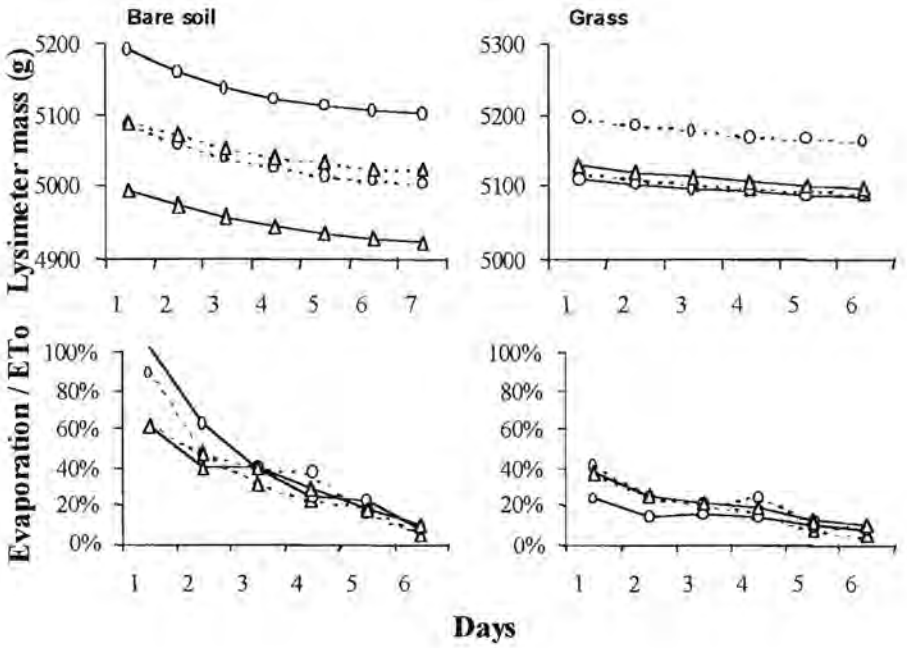

Figure 9. Evaporation from eight micro-lysimeters installed in open field, four of them in a bare soil area, and four of them in a grass-covered area.

The results of this are shown in figure 9. Evaporation appeared to decline from the first day after irrigation. In the bare soil area, the initial values observed during the first day were comparable to *ETo* (60% to 100% of *ETo*), but that was not the case for the lysimeters installed in the grass-covered area, with initial evaporations between 20% and 40% of *ETo*. The fact that the evaporations measured by the micro-lysimeters in the bare soil were lower than *ETo* was probably due to the fact that while the lysimeter surface is made of bare soil, *ETo* is calculated for a grass cover. Also, the fact that the evaporation measured by the lysimeter placed in the grass-covered area was about half as in the bare soil area caused concern. One explanation may be that the grass surrounding the micro-lysimeter (the surface of which was bare) created a micro-climate with lower evaporative demand (lower wind and higher humidity). Another explanation is that the grass that covered the lysimeter was partially dead, acting as a mulch, preventing radiation from reaching the soil surface and increasing the resistance to water movement. The decline in evaporation observed for all micro-lysimeters during the experiment can be described as follows. After irrigation, the soil surface is wet and the evaporation was limited by the net radiation received (energy-limited stage), then the supply of water by the soil to the

surface became limiting and evaporation decreased as the soil became drier (falling rate stage). This behaviour was already reported in previous lysimeter studies (Phillips, 1957). It was modelled by Ritchie (1972) and this model was widely adopted in lysimeter studies (Villalobos and Fereres, 1990; Yanusa et al., 1993).

3.1.3 Lysimeter measurements in the orchard

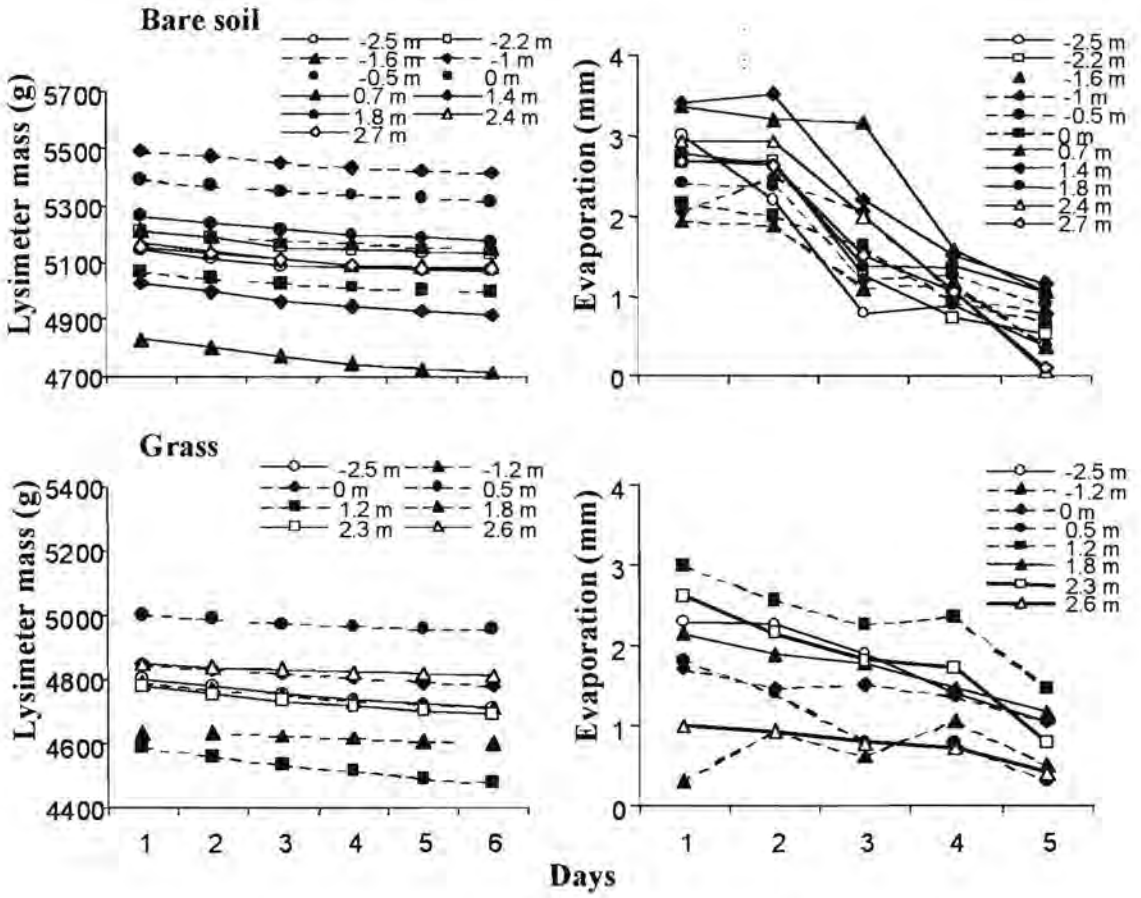

Figure 10. Loss of mass and corresponding evaporation measured by lysimeters installed at several positions in the orchard. One set of lysimeters was in the bare soil area of the orchard, the other set in the grass-covered area. The positions ranged from distances of -2.5 m from the row (southern side of the row) to 2.7 m (northern side) in the bare soil area, and from -2.5 to 2.6 m in the grass-covered area.

The micro-lysimeter measurements made within the orchard reveal important differences in evaporation (Figure 10). The rates of evaporation measured during the first 2 days of the experiment ranged from 1 to 3.5 mm day^{-1}. After the third day, the measured evaporation declined for almost all the lysimeters studied, though the rate

of decline differed between lysimeters: in general, it was higher in the bare soil area than in the grass-covered area, and within a given soil cover, higher for the lysimeters that were far from the row.

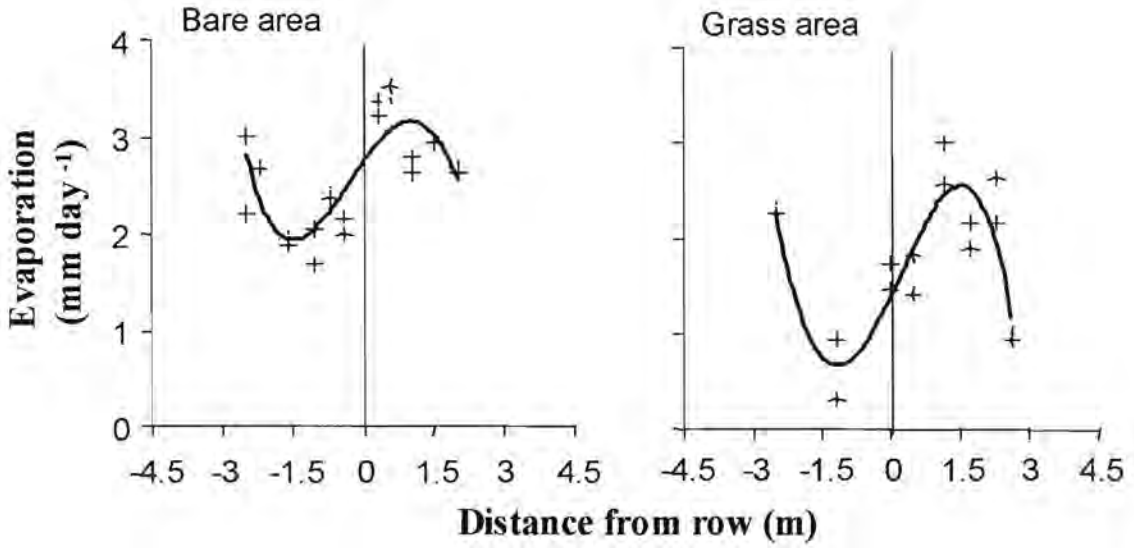

Figure 11. Spatial distribution of evaporation (mm) across the rows. Measured evaporations are expressed in mm day^{-1} and shown for the bare and grass-covered area of the orchard. The values for the distance of the lysimeter from the row (m) are negative for the southern side, positive for the northern side.

For the first two days of measurements, expected to correspond to the energy-limited stage, a clear distribution of evaporation within the row was observed (Figure 11). Evaporation rates appeared to be maximum on the northern side of the row (between 1 and 2 m from the row), and minimum under the trees and on the southern side of the row. This pattern was found both in the bare soil and in the grass-covered area. However, the evaporation rates measured in the grass-covered area was lower than that measured at corresponding positions in the bare soil area.

Relationships between energy interception and evaporation.

The patterns of distribution of evaporation (Figure 11) and cumulative solar energy received daily (Figure 8) being similar, the relations between these two variables were therefore investigated.

A linear correlation between cumulative energy interception and daily evaporation was found for the first 2 days of the experiment (expected to correspond to a situation where evaporation is energy-limited). This correlation was observed for both the bare soil and grass-covered areas (Figure 12). Though the slopes of the regression line were similar, the intersects at the origin were not as evaporation was about 1.2 mm day^{-1} lower in the grass-covered area.

Possible interpretations for the lower rate of evaporation in the grass-covered area are: (i) The grass that covered the soil prevented radiation from reaching the soil surface, thus reducing the amount of energy available for water evaporation at the soil surface; (ii) Grass cover may have created a wetter micro-climate at the soil surface by reducing wind speed and preventing vapour movement by convection.

When measurements for the rest of the experiment (days 3 to 6) were included, the correlation between energy interception and evaporation was lost (data not shown). This suggests that during these days, evaporation was no longer limited by energy interception.

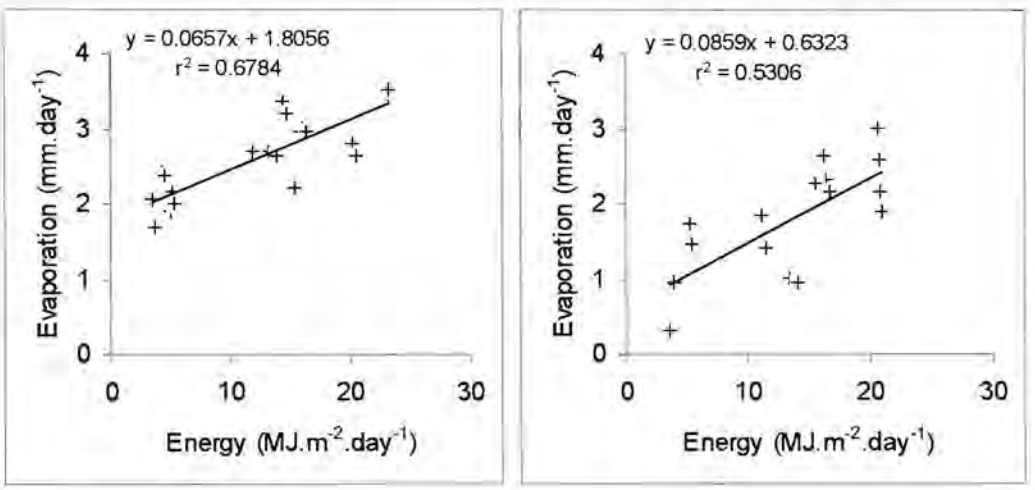

Figure 11. Relation between cumulated daily energy interception and evaporation (bare soil and grass-covered area). Only data from the first 2 days of the experiment are shown.

3.1.4 Validation of the evaporation subroutine

In the "Tree" version of the SWB model, the spatial distribution of evaporation at the soil surface is calculated in two steps:

(i) Potential evaporation (*PE*) is estimated at each node by partitioning potential evapotranspiration (PET) in proportion to the fraction of total above canopy solar energy received locally.

(ii) Evaporation from the soil surface is then modelled as a function of potential evaporation, air humidity, and humidity of the soil surface (as calculated by the 2D model of water redistribution in the soil Campbell (1985).

In the following section, evaporation measurements are compared with both modelled potential evaporation and modelled actual evaporation.

Partitioning of potential evapotranspiration and evaporation measurements

If the evaporation partitioning subroutine predicts potential evapo-transpiration accurately, the following results would be expected:

(i) The ratio between measured evaporation and predicted potential evaporation should remain constant at the beginning of the evaporation measurement when evaporation is expected to be energy-limited, then decline with time as evaporation becomes water-limited.

(ii) The initial ratio should be the same for all micro-lysimeters, as long as the spatial distribution of potential evaporation is predicted accurately. If there is no bias in the calculation of potential evaporation, the ratio should be close to unity.

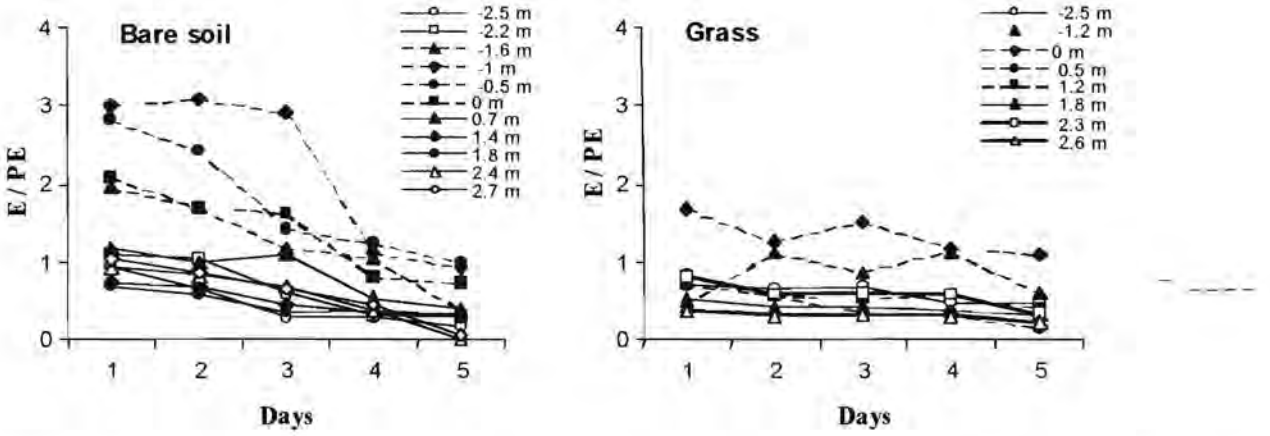

Figure 13. Ratio between evaporation measured by the micro-lysimeters (E) and potential evaporation calculated by the model (PE) at several positions in the orchard. One set of micro-lysimeters was in the bare soil area of the orchard, the other set in the grass-covered area. The positions ranged from distances of -2.5 m from the row (southern side of the row) to 2.7 m (northern side) in the bare soil area, and from -2.5 to 2.6 in the grass-covered area.

For most of the micro-lysimeters, the ratio changed over time as expected (Figure 13). In the bare soil area the ratio was constant or declined little during the first two days, the decline increase during the following days. In the grass area, a slightly different pattern was observed, with the decline starting only after two days of the experiment. These results suggest that evaporation can be considered as limited by energy interception for at least the first two days in both the bare soil and grass covered part of the orchard.

Except for the micro-lysimeters installed on the southern side of the row, most micro-lysimeters installed within a given area gave comparable initial ratios, close to unity in the bare soil area, but closer to 0.5 in the grass-covered area. The difference between the evaporation of bare soil and grass are probably explained by the same reasons as for the preliminary experiment in open field conditions.

Evaporation rates much higher than the predicted potential evaporation, however, were measured by the micro-lysimeters installed on the southern side of the row (between 0 and -1.6 m in the bare soil area, and at 0 and 1.2 m in the grass-covered area). Figure 14 shows the distribution of the discrepancies between the measured evaporation and the potential evaporation predicted by the model during the first two

days of the experiment. A similar pattern appears in the bare soil area and the grass-covered area: measured evaporation is consistently higher than predicted potential evaporation on the southern, shaded side of the row, and lower on the northern, sunny side of the row. This suggests that the predicted evaporation partitioning routine of the model tends to over-estimate the amplitude of the differences in potential evaporation between the shaded and sunny side of the row. This could be due to several factors. Transfers of energy not unaccounted for by the model (e.g. by radiation from the tree to the ground or by convection) may alter the distribution of energy and potential evaporation. Also, the (daily) time step at which the potential evaporation is calculated may be too long in case evaporation becomes water supply-limited during part of the day, it cannot be directly compared with predicted evaporation.

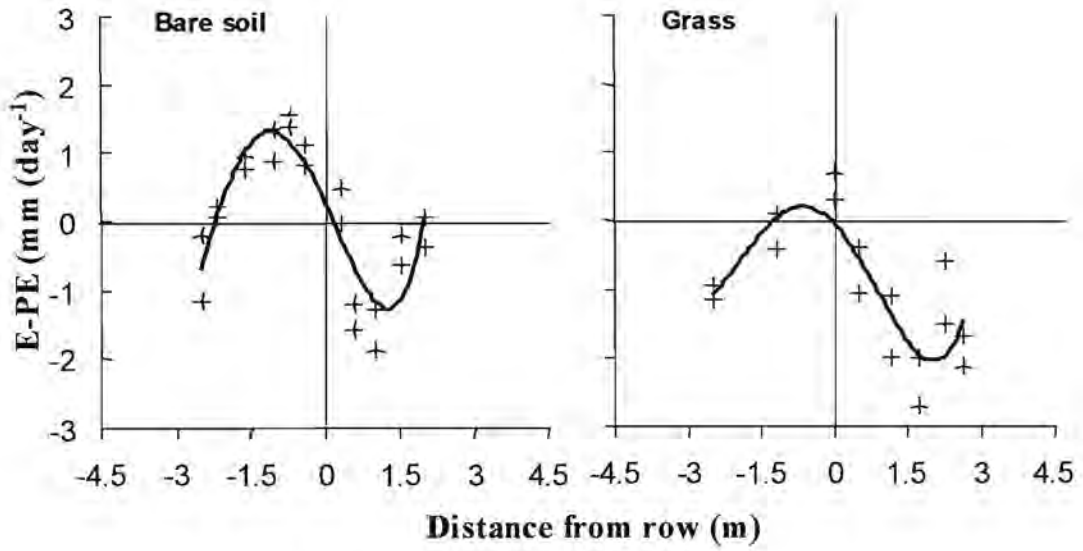

Figure 14. Difference between evaporation measured by lysimeters and potential evaporation calculated by the model (both in mm day^{-1}) in function of the positions in the row. One set of lysimeters was in the bare soil area of the orchard, the other set in the grass-covered area. The positions ranged from distances of -2.5 m from the row (southern side of the row) to 2.7 m (northern side) in the bare soil area, and from -2.5 to 2.6 in the grass-covered area.

Modelled evaporation and lysimeter measurements

When evaporation becomes limited by water supply, it is necessary to know the humidity of the surface layer of the soil to predict it. As no humidity measurements

are possible, the drying of the soil surface had to be simulated using the SWB model. These simulations were set up as follows. Daily cumulative energy interception was simulated as described earlier, and was in excellent agreement with measured values. Evaporation was calculated using the model, setting the horizontal nodes (centres of the evaporation areas) at the lysimeter positions, and the vertical nodes at 1, 2, 3, 6, 26 cm depths, and thereafter every 20 cm.

The first 4 layers described in this set up were therefore 1, 1, 2 and 3 cm thick, which made it possible to describe water distribution close to the surface with accuracy. Due to the way the model is developed, evaporation and distribution of water in the soil could not be simulated independently (that is, measured evaporation could not be used as an input to predict soil humidity). Both were simulated together, using the simulated values of evaporation to predict soil water redistribution, and simulated water redistribution to predict evaporation. One variable used in the model is air humidity. In the current version of the model, air humidity is assumed to be constant and equal to 50 %. Simulations were run with different values for this parameter, ranging from 30% to 70%.

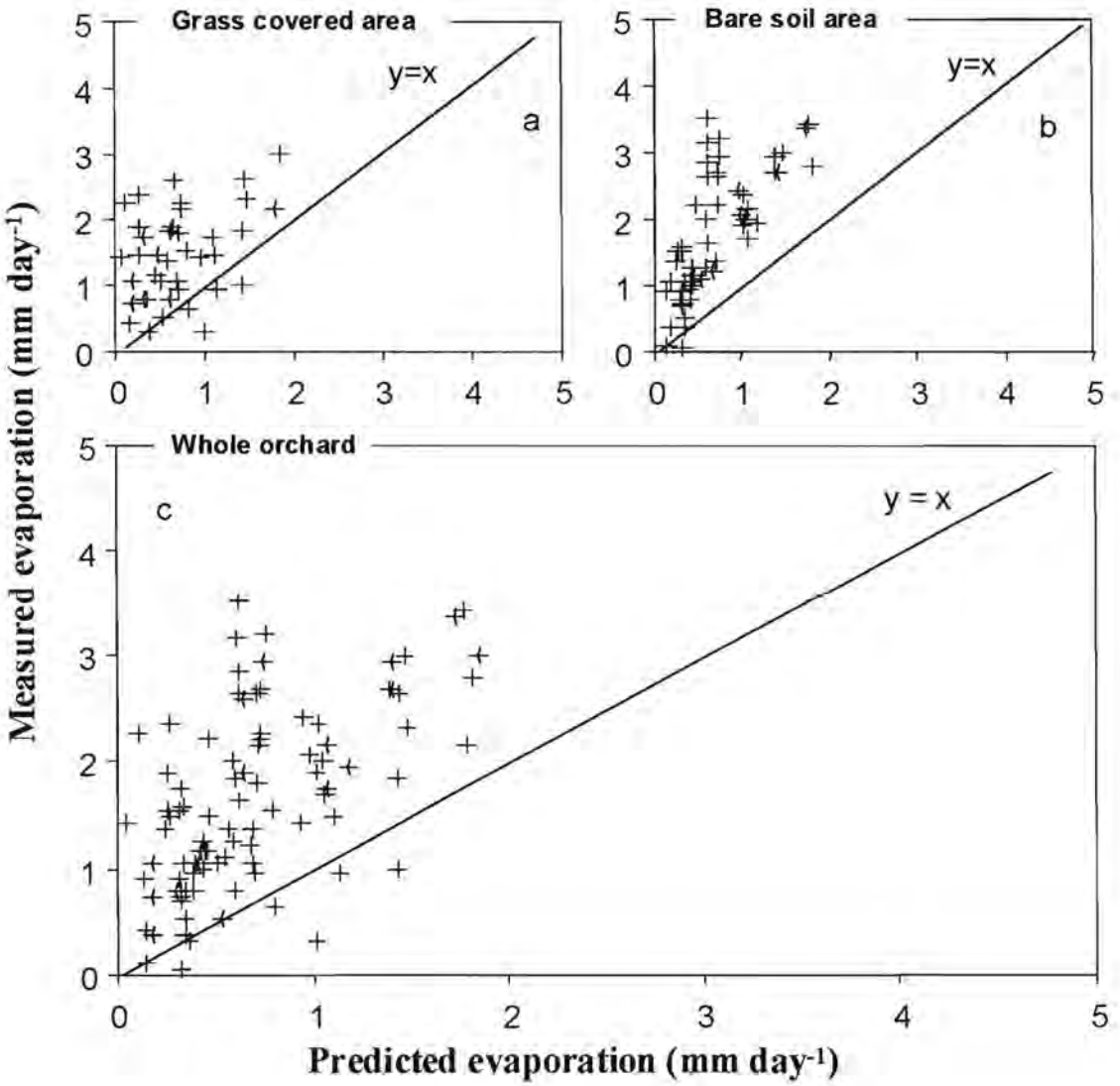

Figure 15. Comparisons between evaporation measured by the micro-lysimeters and predicted by the model. In this simulation, air humidity was assumed to be 50 %, which is the default value in the model.

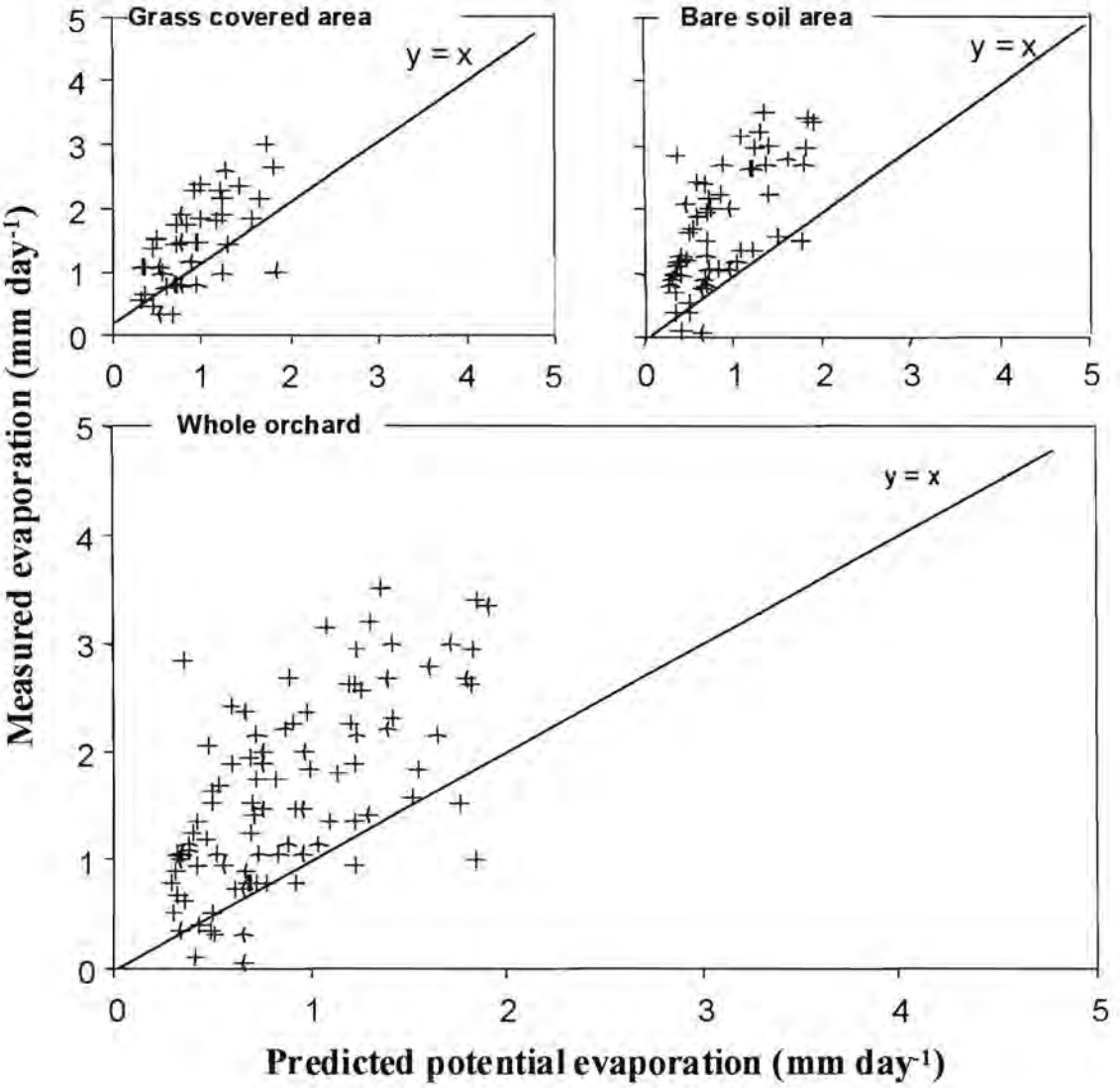

Figure 16. Comparisons between evaporation measured by the micro-lysimeters and predicted by the model. In this simulation, air humidity was assumed to be 30 %, which is the default value in the model.

Simulations assuming 50% air humidity underestimated evaporation grossly (Figure 15). The best agreement was obtained assuming 30 % air humidity (Figure 16). One possible source of error for the model may have been the accuracy in predicting the drying of the soil surface. However, because of lack of experimental data this hypothesis could not be validated. Other sources of errors could have been: (i) The estimation of the parameters of the model, like soil hydraulic conductivity (which was not measured but estimated indirectly from the water contents at field capacity and

permanent wilting point), and (ii) Air humidity (which was taken as constant, while it depends on weather).

Chapter 4

4.1 Conclusion

4.1.1 General comparison between measurements and model predictions.

Simulations of solar radiation interception by the two-dimensional SWB model were in good agreement with observations, though tree dimensions for which the model gave the best predictions were slightly different from those measured in the orchard. Actually, measurements of tree size appeared to be difficult to repeat and were subjective, appropriate guidelines should be established to get repeatable measurements if the model is to be used for extension applications. This problem would become more important when one has to deal with trees with non-symmetric canopies and/or non-uniform leaf distribution. In such cases, significant errors in prediction of solar radiation transmittance are likely to occur. Also, parameters like the leaf area density of the canopy were not measured and may be difficult to estimate.

The simulations of evaporation appeared not to match the measurements with accuracy. This might be due to errors: (i) To the distribution of potential evaporation at the soil surface, (ii) To the humidity of the soil surface layer, and (iii) Calculated evaporation. Inaccuracies in the evaporation measurements using the micro-lysimeter technique are also possible: the experiment conducted in an open field showed that: (i) There was a relatively high variability in lysimeter measurements, even for lysimeters placed in similar conditions; (ii) Evaporation measurements were highly dependent on the local environment (bare soil or grass) in which the micro-lysimeters were installed.

The model seems to overestimate the amplitude of the differences in potential evaporation between the exposed and shaded parts of the soil. This may be due to transfers of energy unaccounted for by the model, e.g. by wind. The part of the model used to predict water distribution in the soil and humidity at the soil surface requires input parameters such as hydraulic conductivity, that could not be measured in this study. Inaccuracies in the soil hydraulic conductivity would cause errors in the

prediction of the humidity of the surface layer of the soil, leading to discrepancies observed between modelled and measured evaporations.

4.1.2 Perspective

Even though further calibration and testing of the SWB model appears advisable to run it routinely as a prediction tool, the present study shows that is based on sound physical principles and gives: (i) Excellent prediction of energy interception patterns, (ii) Satisfying prediction of water use, that could reach a very accurate level with further calibration.

Using the "Tree" version of the SWB model should guide irrigation scheduling consultants, extension officers and farmers to more efficiently use scarce water resources on high value tree crops. The two-dimensional model can also be used for planning purposes as demonstrated in the scenario simulations.

The canopy radiation interception routine will make it possible to evaluate the effect of row orientation and spacing as well as the effect of pruning practices on water use. An optimisation program could be built in SWB in order to optimise all input parameters at the same time. This would facilitate the choice of optimal management without having to run simulations by trial and error.

References

ALLEN, L.H. YOCUM, C.S. & LEMON, E.R., 1964. Photosynthesis under field condition. VII. Radiant energy exchange within a corn crop canopy and implication in water use efficiency. *Agron. J.* 56, 253-259.

ALLEN, G.R, PEREIRA, L.S, RAES, D & SMITH, M. 1998. Crop evapotranspiration. FAO Irrigation and Drainage Paper no.56. FAO. Rome, Italy.

ANNANDALE, J.G, BENADE, N, JOVANOVIC, N.Z, STEYN, J.M, & DU SAUTOY, N, 2000. Facilitating irrigation scheduling by means of the Soil Water Balance model. *Water Research Commission Rep No.* K5/ 753, Pretoria, South Africa.

BEGG, J.E, BURHUZEN, J. F, LEMON, E.R, MISRA, D. K, SLATYER, R.O & STERN, W. R., 1964. Diurnal energy and water exchange in bulrush millet in an area of high solar radiation. *Ag. For. Met.* 1, 294-312.

BENNIE, A.T.P, COETZEE, M.J, VAN ANTWERPEN, R, VAN RENSBURG, L.D & DU T. BURGER R.,1988. N Waterbalansmodel vir besproeiing gesbaseer op profie water voor sieningstempo en gewaswaterbehoeftes. *Waternavorsingskommisie Verslag No.* 144/1/88, Pretoria, South Africa.

BLACK, T.C, TANNER, C.B & GARDNER, W.R., 1970. Evapotranspiration from a snapbean crop. *Agron. J.* 62, 66-69.

BLACK, T.A, GARDNER, W.R. & THURTELL, G.W., 1969. Prediction of evaporation, drainage and soil water storage for a bare soil. *Soil Sci. Soc. Am. Proc.* 33, 655-658.

BOAST, C.W. & ROBERTSON, T.M., 1982. The micro-lysimeter method for determining evaporation from bare soil. Description and laboratory evaluation. *Soil Sci. Soc. Am. J.* 46, 689-696.

BROWN, K.W. & COVEY, C., 1966. The energy-budget evaluation of the micro-meteorological transfer process within a cornfield. *Ag. For. Met.* 3, 73-96.

CAMPBELL, G.S., 1985. Soil physics with Basic. Elsevier Science, Amsterdam.

CAPRIO, J.M, GRUNWALD, G.K, & SNYDER, R.D., 1985. Effect of standing stubble on soil water by evaporation. *Ag. For Met.* 34, 129-144.

CHARLES - EDWARDS, D.A. & THORNLEY, H.M. (1973). Light interception by an isolated plant. A simple model. *Ann. Bot.* 37, 919-928.

CHARLES – EDWARDS, D.A. & THORPE, M.R. (1976). Interception of diffuse and direct – beam radiation by a hedgerow apple orchard. *Ann. Bot.* 40, 603 – 613.

CROSBY, C.T., 1996. SAPWAT 1.0 - A computer program for estimating irrigation requirements in Southern Africa. *Water Research Commission Rep No.* 379/1/96, Pretoria, South Africa.

DOUD, D.S. & FERREE, D.C., 1980. Influence of altered light levels on growth and fruiting of mature delicious apple trees. *Am. J. Soc. Hortic. Sci.*105, 325-328.

FUCHS, M., 1972. The control of the radiation climate of plant communities. In. D. Hillel (Ed), Optimizing the Soil Physical Environment toward Greater Crop Yields. *Academic Press, New York.* 173-191.

HAM, J.M, HEILMAN, J.L, & LASCANO, RJ., 1991. Soil and canopy energy balances of a row crop at partial cover. *Agron. J.* 83, 744-753.

LASCANO, R.J, & VAN BAVEL, C.H.M. 1986. Simulation and measurement of evaporation from a bare soil. *Soil Sci. Soc. Am. J.* 50, 1127-1132.

LASCANO, R.J, VAN BAVEL, C.H.M, HATFIELD, J.L. & UPCHURCH, D.R., 1987. Energy and water balance of a sparse crop: Simulated and measured soil and crop evaporation. *Soil Sci. Soc. Am. J.* 51, 1113-1121.

MATTHIAS, A.D., SALEHI, R. & WARRICK, A.N., 1986. Bare soil evaporation near a surface point- source emitter. *Agric. Water Manage.* 11, 257-277.

MONTEITH, J.L., 1977. Climate and efficiency of crop production in Britain. *Philos. Trans. R. Soc. London, Ser. B* 281, 277-294.

MORGAN, D.C., STANLEY, C. J., VOLTZ, R., & WARRINGTON, I. L., 1984. Summer pruning of Gala apple: the relationships between pruning time, radiation penetration, and fruit quality. *Am. J. Soc. Hortic. Sci.* 109, 637-642.

PENMAN, H.L., 1948. Natural evaporation from open water, bare soil and grass. *Proc R. Soc. London (A).* 193, 120-145.

PHILLIP, R.J., 1957. Evaporation, moisture and heat fields in the soil. *Ag. For. Met.* 14, 354-366.

PRUITT, W.D, HENDERSON, W.D, FERERES, E, HAGAN, R.M, MARTIN, P.E, TARANTINO, E, SINGH, H, CHANDIO, B., 1984. Micro-climate, evapotranspiration, and water use efficiency for drip-irrigation tomatoes. *Transactions of the 12th Congress International Committee on Irrigation and* Drainage (A), 367-394.

RITCHIE, J.T., 1972. Model for predicting evaporation from a row crop with incomplete cover. *Water Resour. Res.* 8, 1204-1213.

SHAWCROFT, R.W. & GARDNER, H.R., 1983. Direct evaporation from soil under a row canopy. *Ag. For Met.* 28, 229-239.

SHUTTLEWORTH, J.W & WALLACE, J.S., 1985. Evaporation from sparse crops – an energy combination theory. *Quat. Jor. Roy. Met. Soc.*111, 839-855.

SINCLAIR, T.R & SELIGMAN, N.S., 1996. Crop modeling from infancy to maturity. *Agron. J.* 88, 698-704.

SMITH, M., 1992b. Expert consultation on reversion of FAO methodology for crop water requirements. *Proc. of the Int. Conf. on Evapotranspiration and irrigation Scheduling*. San Antonio, Texas, USA. 133-140.

SOIL CLASSIFICATION WORKING GROUP (1991) Soil classification. A taxonomic system for South Africa. Dept of Agricultural Development, Pretoria, South Africa.

STEINER, J.L., 1989. Tillage and surface residue effects on evaporation from soils. *Soil Sci. Soc Am. J.* 53, 911-916.

TANNER, C.B., 1960. Energy balance approach to evapotranspiration from crops. *Soil. Sci. Soc. Am. Proc.* 24, 1-9.

TANNER, C.B. & JURY, W.A., 1976. Estimating evaporation and transpiration from a row crop during incomplete cover. *Agron. J.* 68, 239-243.

VILLALOBOS, F.J & FERERES, E., 1990. Evaporation measurement beneath corn, cotton and sunflower canopies. *Agron. J.* 82, 1153-1159.

WALKER, G.K., 1984. Development and validation of a numerical model simulating evaporation from short cores. *Soil Sci. Soc. Am. J.* 48, 960-969.

YANUSA, I.A.M, SEDGLEY, R.H, BELFORD, R.K & TENNANT, D., 1993. Dynamics of water use in a Mediterranean environment. I. Soil evaporation little affected by presence of plant canopies. *Agric Water Manage* 24, 205-224.

Appendix 1: Wiring table of the seven solarimeter tubes.

Solarimeters no	Logger channels	Battery connection
1	H_3 (red) and G (grey)	Red (+) and Blue (-)
2	L_3 (red) and G (grey)	
3	H_3 (red) and G (grey)	
4	L_4 (red) and G (grey)	
5	H_5 (red) and G (grey)	
6	L_5 (red) and G (grey)	
7	H_6 (red) and G (grey)	

Note: All wires with transparent insulation from solarimeter tubes connected to ground on datalogger.

Appendix 2: Logger program of the solarimeter tubes

```
;{CR10}
'
*Table 1 Program
  01: 10       Execution Interval (seconds)

1: Batt Voltage (P10)
 1: 1        Loc [ Battery   ]

2: Volt (SE) (P1)
 1: 1        Reps
 2: 23       25 mV 60 Hz Rejection Range
 3: 1        SE Channel
 4: 2        Loc [ Solar1    ]
 5: 85.891   Mult
 6: -6.55    Offset

3: Volt (SE) (P1)
 1: 1        Reps
 2: 23       25 mV 60 Hz Rejection Range
 3: 2        SE Channel
 4: 3        Loc [ Solar2    ]
 5: 87.45    Mult
 6: -12.793  Offset

4: Volt (SE) (P1)
 1: 1        Reps
 2: 23       25 mV 60 Hz Rejection Range
 3: 3        SE Channel
 4: 4        Loc [ Solar3    ]
 5: 85.791   Mult
 6: -3.515   Offset

5: Volt (SE) (P1)
 1: 1        Reps
 2: 23       25 mV 60 Hz Rejection Range
 3: 4        SE Channel
 4: 5        Loc [ Solar4    ]
 5: 87.503   Mult
 6: -1.3003  Offset

6: Volt (SE) (P1)
 1: 1        Reps
 2: 23       25 mV 60 Hz Rejection Range
 3: 5        SE Channel
 4: 6        Loc [ Solar5    ]
 5: 83.811   Mult
 6: -3.3513  Offset

7: Volt (SE) (P1)
```

```
 1: 1        Reps
 2: 23       25 mV 60 Hz Rejection Range
 3: 6        SE Channel
 4: 7        Loc [ Solar6    ]
 5: 84.75    Mult
 6: -2.1387  Offset

 8:  Volt (SE) (P1)
  1: 1       Reps
  2: 23      25 mV 60 Hz Rejection Range
  3: 7       SE Channel
  4: 8       Loc [ Solar7    ]
  5: 1.0     Mult
  6: 0.0     Offset

 9:  If time is (P92)
  1: 0       Minutes (Seconds --) into a
  2: 5       Interval (same units as above)
  3: 10      Set Output Flag High

 10:  Set Active Storage Area (P80)
  1: 1       Final Storage Area 1
  2: 222     Array ID

 11:  Real Time (P77)
  1: 1220    Year,Day,Hour/Minute (midnight = 2400)

 12:  Sample (P70)
  1: 8       Reps
  2: 1       Loc [ Battery   ]

*Table 2 Program
  02: 0.0000    Execution Interval (seconds)

*Table 3 Subroutines

End Program

-Input Locations-
1 Battery   5 1 1
2 Solar1    9 1 1
3 Solar2    9 1 1
4 Solar3    9 1 1
5 Solar4    9 1 1
6 Solar5    9 1 1
7 Solar6    9 1 1
8 Solar7    17 1 1
9 _____ 1 0 0
10 _____ 1 0 0
11 _____ 0 0 0
12 _____ 0 0 0
13 _____ 0 0 0
14 _____ 0 0 0
15 _____ 0 0 0
```

16 _____ 0 0 0
17 _____ 0 0 0
18 _____ 0 0 0
19 _____ 0 0 0
20 _____ 0 0 0
21 _____ 0 0 0
22 _____ 0 0 0
23 _____ 0 0 0
24 _____ 0 0 0
25 _____ 0 0 0
26 _____ 0 0 0
27 _____ 0 0 0
28 _____ 0 0 0
-Program Security-
0
0
0
-Mode 4-
-Final Storage Area 2-
0

Appendix 3: Wiring table of the automatic weather station.

Equipment	Logger channels	Battery connection
Pyranometer	H_3 (blue) and L_4 (red)	Red(+) and Blue(-)
Rain gauge	P_2 (red) and G (blue)	
Anemometer	H_5 (orange) and L_6 (white)	
Temp & Humidity	E_2 (white) and E_2 (pink)	

Appendix 4: Logger program of the automatic weather station

```
;{CR10X}
*Table 1 Program
  01: 10.0000   Execution Interval (seconds)

1:  Temp (107) (P11)
  1: 1        Reps
  2: 1        SE Channel
  3: 1        Excite all reps w/E1
  4: 1        Loc [ Temp      ]
  5: 1        Mult
  6: .17      Offset

2:  Excite-Delay (SE) (P4)
  1: 1        Reps
  2: 5        2500 mV Slow Range
  3: 2        SE Channel
  4: 2        Excite all reps w/Exchan 2
  5: 15       Delay (units 0.01 sec)
  6: 2500     mV Excitation
  7: 2        Loc [ Humidity  ]
  8: .1028    Mult
  9: 1.42     Offset

3:  Pulse (P3)
  1: 1        Reps
  2: 1        Pulse Channel 1
  3: 21       Low Level AC, Output Hz
  4: 3        Loc [ Wind      ]
  5: 0.098    Mult
  6: 0.001    Offset

4:  Volt (Diff) (P2)
  1: 1        Reps
  2: 33       25 mV 50 Hz Rejection Range
  3: 2        DIFF Channel
  4: 4        Loc [ Radiation ]
  5: 120.21   Mult
  6: -24.388  Offset

5:  Pulse (P3)
  1: 1        Reps
  2: 2        Pulse Channel 2
  3: 2        Switch Closure, All Counts
  4: 5        Loc [ Rain      ]
  5: .4976    Mult
  6: 0        Offset

6:  Z=X*F (P37)
  1: 2        X Loc [ Humidity  ]
  2: .01      F
```

```
3: 7       Z Loc [ HumFrac   ]

7:  Saturation Vapor Pressure (P56)
 1: 1       Temperature Loc [ Temp      ]
 2: 8       Loc [ SVP       ]

8:  Z=X*Y (P36)
 1: 8       X Loc [ SVP       ]
 2: 7       Y Loc [ HumFrac   ]
 3: 9       Z Loc [ VP        ]

9:  Z=X-Y (P35)
 1: 8       X Loc [ SVP       ]
 2: 9       Y Loc [ VP        ]
 3: 10      Z Loc [ VPD       ]

10:  Batt Voltage (P10)
 1: 6       Loc [ Battery   ]

11:  If time is (P92)
 1: 0       Minutes (Seconds --) into a
 2: 60      Interval (same units as above)
 3: 10      Set Output Flag High (Flag 0)

12:  Real Time (P77)
 1: 1220    Year,Day,Hour/Minute (midnight = 2400)

13:  Average (P71)
 1: 2       Reps
 2: 1       Loc [ Temp      ]

14:  Maximum (P73)
 1: 1       Reps
 2: 00      Time Option
 3: 2       Loc [ Humidity  ]

15:  Minimum (P74)
 1: 1       Reps
 2: 00      Time Option
 3: 2       Loc [ Humidity  ]

16:  Average (P71)
 1: 2       Reps
 2: 3       Loc [ Wind      ]

17:  Totalize (P72)
 1: 1       Reps
 2: 5       Loc [ Rain      ]

18:  Average (P71)
 1: 3       Reps
 2: 8       Loc [ SVP       ]

19:  If time is (P92)
```

```
 1: 0       Minutes (Seconds --) into a
 2: 1440    Interval (same units as above)
 3: 10      Set Output Flag High (Flag 0)

20: Real Time (P77)
 1: 1200    Year,Day (midnight = 2400)

21: Average (P71)
 1: 1       Reps
 2: 1       Loc [ Temp     ]

22: Maximum (P73)
 1: 1       Reps
 2: 10      Value with Hr-Min
 3: 1       Loc [ Temp     ]

23: Minimum (P74)
 1: 1       Reps
 2: 10      Value with Hr-Min
 3: 1       Loc [ Temp     ]

24: Maximum (P73)
 1: 1       Reps
 2: 10      Value with Hr-Min
 3: 2       Loc [ Humidity ]

25: Minimum (P74)
 1: 1       Reps
 2: 10      Value with Hr-Min
 3: 2       Loc [ Humidity ]

26: Average (P71)
 1: 2       Reps
 2: 3       Loc [ Wind     ]

27: Totalize (P72)
 1: 1       Reps
 2: 5       Loc [ Rain     ]

28: Minimum (P74)
 1: 1       Reps
 2: 00      Time Option
 3: 6       Loc [ Battery  ]

29: Average (P71)
 1: 3       Reps
 2: 8       Loc [ SVP      ]

*Table 2 Program
  01: 0.0000    Execution Interval (seconds)

*Table 3 Subroutines

End Program
```

-Input Locations-
1 Temp 1 5 1
2 Humidity 1 6 1
3 Wind 1 2 1
4 Radiation 1 2 1
5 Rain 1 2 1
6 Battery 1 1 1
7 HumFrac 1 1 1
8 SVP 1 4 1
9 VP 1 3 1
10 VPD 1 2 1
11 _____ 0 0 0
12 _____ 0 0 0
13 _____ 0 0 0
14 _____ 0 0 0
15 _____ 0 0 0
16 _____ 0 0 0
17 _____ 0 0 0
18 _____ 0 0 0
19 _____ 0 0 0
20 _____ 0 0 0
21 _____ 0 0 0
22 _____ 0 0 0
23 _____ 0 0 0
24 _____ 0 0 0
25 _____ 0 0 0
26 _____ 0 0 0
27 _____ 0 0 0
28 _____ 0 0 0
-Program Security-
0
0
0
-Mode 4-
-Final Storage Area 2-
0
-CR10X ID-
0
-CR10X Power Up-
3

Appendix 5: Weather data

Year	DOY	Hour	Temp (°C)	RH (%)	Max RH (%)	Min RH (%)	Wind ($m.s^{-1}$)	Radiation ($W.m^{-2}$)	Rain (mm)	SVP (kPa)	VP (kPa)	VPD (kPa)
2001	64	100	19.5	71	76	66	0.0	0	0	2.26	1.61	0.66
2001	64	200	19.1	74	77	71	0.0	0	0	2.21	1.64	0.57
2001	64	300	18.4	79	82	76	0.0	0	0	2.11	1.67	0.44
2001	64	400	17.9	84	89	81	0.0	0	0	2.05	1.71	0.34
2001	64	500	16.6	91	95	89	0.0	0	0	1.89	1.72	0.17
2001	64	600	16.1	96	97	94	0.0	0	0	1.83	1.75	0.08
2001	64	700	16.4	96	98	94	0.0	0	0	1.86	1.79	0.07
2001	64	800	18.2	89	95	84	0.0	262	0	2.10	1.86	0.23
2001	64	800	19.9	84	86	83	1.8	468	0	2.32	1.96	0.37
2001	64	900	21.0	80	85	75	1.6	605	0	2.48	1.99	0.50
2001	64	1000	22.7	75	79	70	1.4	812	0	2.75	2.05	0.70
2001	64	1100	23.9	68	78	59	1.4	920	0	2.97	2.01	0.96
2001	64	1200	25.6	59	68	52	1.4	1030	0	3.28	1.93	1.36
2001	64	1300	27.0	52	61	46	1.4	990	0	3.56	1.84	1.72
2001	64	1400	28.2	41	54	36	1.9	915	0	3.82	1.56	2.26
2001	64	1500	29.0	37	46	34	1.7	783	0	4.00	1.50	2.50
2001	64	1600	28.9	36	42	33	1.7	510	0	3.98	1.43	2.55
2001	64	1700	28.5	38	42	34	1.4	288	0	3.90	1.47	2.42
2001	64	1800	27.4	48	57	37	1.3	119	0	3.66	1.75	1.91
2001	64	1900	24.3	64	69	56	0.5	0	0	3.04	1.94	1.10
2001	64	2000	22.7	72	75	68	0.3	0	0	2.75	1.97	0.78
2001	64	2100	21.6	75	78	73	0.3	0	0	2.57	1.92	0.65
2001	64	2200	20.7	76	79	73	0.4	0	0	2.43	1.85	0.58
2001	64	2300	20.1	76	81	72	0.6	0	0	2.36	1.79	0.56
2001	64	2400	20.1	74	77	71	0.8	0	0	2.35	1.75	0.60
2001	65	100	19.3	79	81	73	0.8	0	0	2.24	1.76	0.48
2001	65	200	18.9	86	89	79	1.2	0	0	2.18	1.87	0.31
2001	65	300	18.2	92	95	89	1.2	0	0	2.09	1.92	0.17
2001	65	400	17.8	96	98	95	1.2	0	0	2.03	1.96	0.08
2001	65	500	17.4	99	100	97	1.2	0	0	1.99	1.97	0.02
2001	65	600	17.3	100	101	100	1.1	0	0	1.97	1.98	0.00
2001	65	700	17.8	100	102	97	1.0	103	0	2.04	2.04	0.00
2001	65	800	20.2	92	97	86	0.8	376	0	2.37	2.18	0.19
2001	65	900	21.7	85	89	80	0.9	602	0	2.60	2.21	0.38
2001	65	100	23.3	77	83	72	0.8	724	0	2.85	2.19	0.66
2001	65	1100	24.9	68	79	61	1.0	970	0	3.14	2.14	1.01
2001	65	1200	27.0	58	66	54	1.1	1017	0	3.56	2.08	1.48
2001	65	1300	28.3	52	62	45	1.2	982	0	3.84	2.01	1.83
2001	65	1400	29.4	48	58	40	1.3	956	0	4.11	1.95	2.15
2001	65	1500	30.3	37	50	32	1.7	801	0	4.31	1.59	2.72
2001	65	1600	30.4	37	42	34	1.9	574	0	4.33	1.60	2.73
2001	65	1700	29.8	37	46	33	1.5	267	0	4.20	1.57	2.63
2001	65	1800	29.0	40	49	35	1.0	100	0	4.00	1.59	2.41
2001	65	1900	25.2	62	72	47	0.5	0	0	3.21	1.99	1.22
2001	65	2000	23.3	70	75	66	0.6	0	0	2.86	2.00	0.85
2001	65	2100	23.3	70	78	66	1.4	0	0	2.86	1.99	0.88
2001	65	2200	22.6	73	81	66	1.0	0	0	2.75	1.98	0.76

2001	65	2300	20.9	75	88	63	1.1	0	0	2.48	1.86	0.62
2001	65	2400	20.1	74	81	65	0.6	0	0	2.35	1.74	0.61
2001	66	100	18.5	81	86	73	1.0	0	0	2.13	1.73	0.40
2001	66	200	18.9	73	76	71	2.6	0	0	2.18	1.59	0.59
2001	66	300	17.9	78	81	74	1.7	0	0	2.05	1.60	0.45
2001	66	400	17.6	83	87	80	2.0	0	0	2.01	1.68	0.34
2001	66	500	17.4	90	93	87	1.9	0	0	1.98	1.78	0.20
2001	66	600	17.1	94	96	93	2.1	0	0	1.95	1.84	0.11
2001	66	700	17.8	92	95	88	2.3	99	0	2.04	1.88	0.16
2001	66	800	20.4	84	89	78	2.4	355	0	2.40	2.01	0.39
2001	66	900	22.5	78	82	74	2.6	600	0	2.73	2.13	0.60
2001	66	1000	24.5	71	78	64	2.6	816	0	3.08	2.18	0.89
2001	66	1100	25.8	62	70	53	2.6	838	0	3.33	2.06	1.27
2001	66	1200	27.2	47	62	37	2.1	1038	0	3.61	1.71	1.90
2001	66	1300	28.1	41	50	35	2.0	1027	0	3.80	1.54	2.26
2001	66	1400	28.8	39	47	35	1.6	949	0	3.96	1.54	2.42
2001	66	1500	29.4	38	46	34	1.4	789	0	4.09	1.55	2.54
2001	66	1600	29.8	39	49	34	1.3	591	0	4.20	1.62	2.57
2001	66	1700	29.5	40	46	35	1.2	360	0	4.12	1.64	2.48
2001	66	1800	28.1	47	54	37	0.9	99	0	3.80	1.77	2.04
2001	66	1900	24.9	60	68	52	0.5	0	0	3.16	1.89	1.26
2001	66	2000	23.4	66	71	63	0.4	0	0	2.88	1.89	0.99
2001	66	2100	22.1	69	73	65	0.4	0	0	2.65	1.83	0.82
2001	66	2200	21.7	68	73	63	0.6	0	0	2.59	1.76	0.83
2001	66	2300	21.6	70	75	64	1.6	0	0	2.59	1.81	0.77
2001	66	2400	20.6	76	82	71	1.5	0	0	2.42	1.83	0.59
2001	67	100	19.8	85	88	82	1.5	0	0	2.31	1.97	0.34
2001	67	200	19.8	92	95	88	1.8	0	0	2.31	2.12	0.18
2001	67	300	19.3	98	100	95	1.2	0	0	2.24	2.20	0.05
2001	67	400	18.8	101	102	100	1.0	0	0	2.16	2.18	-0.02
2001	67	500	18.1	102	104	101	0.6	0	0	2.07	2.11	-0.04
2001	67	600	17.7	104	105	103	0.5	0	0	2.02	2.10	-0.08
2001	67	700	18.1	105	106	103	0.4	76	0	2.07	2.17	-0.10
2001	67	800	20.8	97	104	89	0.7	332	0	2.46	2.38	0.08
2001	67	900	22.5	87	91	84	0.9	580	0	2.72	2.38	0.35
2001	67	1000	23.6	83	88	78	1.1	724	0	2.91	2.42	0.49
2001	67	1100	25.0	77	83	69	1.5	853	0	3.17	2.45	0.72
2001	67	1200	26.3	72	79	66	1.6	829	0	3.42	2.48	0.94
2001	67	1300	27.3	68	76	58	2.1	894	0	3.64	2.46	1.18
2001	67	1400	28.1	65	70	57	2.0	727	0	3.80	2.45	1.35
2001	67	1500	29.1	59	66	53	1.4	538	0	4.02	2.38	1.64
2001	67	1600	24.4	77	85	53	1.8	179	1.0	3.06	2.35	0.71
2001	67	1700	25.0	68	77	61	0.9	221	0	3.17	2.15	1.02
2001	67	1800	24.6	73	82	68	0.7	17	0	3.08	2.25	0.84
2001	67	1900	23.4	80	86	75	0.6	0	0	2.87	2.28	0.59
2001	67	2000	22.0	87	95	81	0.7	0	0	2.65	2.30	0.35
2001	67	2100	22.0	87	92	81	0.4	0	0	2.65	2.30	0.35
2001	67	2200	21.1	92	96	84	0.5	0	0	2.51	2.30	0.21
2001	67	2300	20.2	96	101	84	0.5	0	0	2.37	2.26	0.11
2001	67	2400	20.5	94	100	89	1.1	0	0	2.41	2.26	0.15

2001	68	100	19.6	97	100	92	1.1	0	0	2.28	2.21	0.07
2001	68	200	20.4	85	94	78	1.5	0	0	2.40	2.04	0.37
2001	68	300	19.5	85	88	82	1.0	0	0	2.26	1.92	0.34
2001	68	400	19.4	89	90	88	1.9	0	0	2.25	1.99	0.26
2001	68	500	19.4	92	93	90	2.9	0	0	2.25	2.07	0.19
2001	68	600	18.9	94	96	92	2.2	0	0	2.18	2.05	0.13
2001	68	700	18.8	93	96	90	2.2	80	0	2.17	2.01	0.16
2001	68	800	20.9	86	91	81	2.4	330	0	2.48	2.12	0.36
2001	68	900	22.7	82	84	78	2.5	562	0	2.75	2.24	0.51
2001	68	1000	24.0	73	81	65	2.5	749	0	2.98	2.17	0.82
2001	68	1100	25.5	66	71	62	2.1	907	0	3.27	2.16	1.11
2001	68	1200	26.8	62	69	56	1.8	991	0	3.53	2.18	1.35
2001	68	1300	28.2	54	65	46	1.4	1012	0	3.83	2.06	1.77
2001	68	1400	29.1	52	61	45	1.3	916	0	4.03	2.08	1.95
2001	68	1500	29.9	49	57	43	1.0	838	0	4.23	2.05	2.18
2001	68	1600	30.1	49	57	43	1.4	636	0	4.27	2.07	2.19
2001	68	1700	29.0	51	59	46	0.9	161	0	4.01	2.04	1.97
2001	68	1800	27.5	59	63	55	0.7	66	0	3.68	2.15	1.52
2001	68	1900	25.5	66	68	61	0.6	0	0	3.26	2.14	1.12
2001	68	2000	23.9	71	76	67	0.8	0	0	2.97	2.12	0.85
2001	68	2100	21.6	79	83	74	0.3	0	0	2.58	2.03	0.55
2001	68	2200	20.6	83	87	79	0.6	0	0	2.43	2.02	0.41
2001	68	2300	21.9	76	86	71	1.2	0	0	2.63	1.99	0.63
2001	68	2400	22.3	76	77	75	2.7	0	0	2.69	2.04	0.65
2001	69	100	21.7	77	80	76	2.5	0	0	2.59	2.00	0.59
2001	69	200	20.9	87	99	80	1.8	0	5.0	2.47	2.14	0.34
2001	69	300	18.6	102	103	99	1.8	0	3.0	2.14	2.18	-0.04
2001	69	400	18.8	102	104	101	1.5	0	0	2.16	2.22	-0.05
2001	69	500	18.8	104	104	103	1.2	0	0	2.16	2.24	-0.08
2001	69	600	18.2	104	105	104	0.8	0	0	2.10	2.19	-0.09
2001	69	700	18.5	104	105	103	0.9	26	0	2.13	2.22	-0.09
2001	69	800	20.1	100	104	97	0.6	165	0	2.35	2.34	0.01
2001	69	900	21.2	94	100	90	0.9	442	0.5	2.52	2.38	0.15
2001	69	1000	22.6	89	94	84	1.9	674	0	2.74	2.44	0.31
2001	69	1100	23.7	85	89	79	2.1	688	0	2.92	2.48	0.45
2001	69	1200	24.7	79	83	72	2.6	711	0	3.11	2.45	0.66
2001	69	1300	25.5	73	79	67	2.6	752	0	3.25	2.38	0.87
2001	69	1400	26.2	70	75	66	2.3	619	0	3.40	2.39	1.01
2001	69	1500	27.0	66	71	61	2.3	646	0	3.57	2.36	1.22
2001	69	1600	27.3	63	69	58	2.6	555	0	3.63	2.27	1.35
2001	69	1700	27.1	62	67	57	1.9	350	0	3.58	2.22	1.36
2001	69	1800	26.1	66	71	61	1.4	54	0	3.38	2.22	1.16
2001	69	1900	23.6	76	81	70	1.5	0	0	2.91	2.22	0.69
2001	69	2000	21.8	83	85	79	1.6	0	0	2.61	2.16	0.46
2001	69	2100	21.2	82	87	74	1.1	0	0	2.51	2.07	0.44
2001	69	2200	21.5	79	85	76	1.7	0	0	2.57	2.01	0.55
2001	69	2300	21.2	81	86	78	1.0	0	0	2.52	2.05	0.47
2001	69	2400	20.2	86	91	84	0.4	0	0	2.37	2.04	0.33
2001	70	100	19.9	90	95	85	1.1	0	0	2.33	2.08	0.25
2001	70	200	19.5	92	95	85	0.8	0	0	2.27	2.09	0.17
2001	70	300	18.6	96	98	93	0.9	0	0	2.15	2.05	0.09
2001	70	400	18.3	97	99	97	1.1	0	0	2.10	2.04	0.06

2001	70	500	17.7	99	100	97	1.0	0	0	2.02	1.99	0.03
2001	70	600	17.5	98	99	97	1.4	0	0	2.00	1.97	0.04
2001	70	700	17.9	95	97	94	3.6	0	0	2.05	1.95	0.10
2001	70	800	19.2	92	96	87	3.9	253	0	2.23	2.05	0.18
2001	70	900	20.7	87	89	83	3.1	281	0	2.44	2.11	0.33
2001	70	1000	23.0	79	85	72	2.0	639	0	2.81	2.20	0.60
2001	70	1100	25.5	70	77	65	1.3	966	0	3.27	2.29	0.98
2001	70	1200	26.4	66	74	58	1.6	1034	0	3.44	2.26	1.18
2001	70	1300	27.5	61	69	51	1.7	1026	0	3.66	2.23	1.43
2001	70	1400	28.1	54	63	41	1.8	861	0	3.80	2.06	1.74
2001	70	1500	28.8	46	54	38	2.1	807	0	3.95	1.81	2.14
2001	70	1600	29.0	42	48	37	1.7	609	0	4.00	1.67	2.33
2001	70	1700	28.8	41	46	38	1.3	367	0	3.95	1.63	2.33
2001	70	1800	27.6	44	50	40	1.2	106	0	3.69	1.61	2.08
2001	70	1900	24.7	53	58	49	0.8	0	0	3.11	1.66	1.45
2001	70	2000	23.7	59	63	54	0.8	0	0	2.93	1.72	1.22
2001	70	2100	23.2	59	62	57	1.0	0	0	2.84	1.67	1.17
2001	70	2200	22.4	62	66	58	1.0	0	0	2.70	1.67	1.04
2001	70	2300	21.6	67	71	64	1.1	0	0	2.58	1.73	0.84
2001	70	2400	20.4	73	81	69	0.6	0	0	2.39	1.75	0.64